

Time-Resolved Resonance Raman Spectroscopic Investigation of the *trans*-Stilbene Cation Radical Kinetics in Photolytically Induced Electron-Transfer Reactions

Walter Hub, Ulrich Klüter, Siegfried Schneider, Friedrich Dörr,*

Institut für Physikalische und Theoretische Chemie, Technische Universität München, D-8046 Garching, West Germany

Joe D. Oxman, and Frederick D. Lewis*

Department of Chemistry, Northwestern University, Evanston, Illinois 60201 (Received: August 10, 1983)

The formation of the *trans*-stilbene cation radical in photoreactions involving *trans*-stilbene and the electron-acceptor molecules fumaronitrile, 9-cyanoanthracene, and 9,10-dicyanoanthracene in acetonitrile solution at room temperature is established by the observation of identical transient resonance Raman (TR³) spectra. The excitation profile of the resonance Raman bands closely follows the electronic spectrum of the *trans*-stilbene radical cation. The decay kinetics of the Raman band intensities measured under various experimental conditions give evidence for two reactions, which are competitive with the homogeneous recombination of the *trans*-stilbene cation radical with the corresponding radical anion: (i) recombination with a fumaronitrile dimer anion radical and (ii) recombination with superoxide ion to yield oxidation products. *trans*-Stilbene is one of the first molecules for which the resonance Raman spectra of its short-lived cation and anion radical in the same solvent are now known. In contrast to the electronic absorption spectra, the resonance Raman spectra of the two radical ions are significantly different.

Introduction

The resonance Raman (RR) spectra of a number of short-lived ion radicals in solution have been reported in the past few years under various conditions of formation,¹ including chemical reactions,² photolysis,³ electron pulse radiolysis,⁴ or electrolysis.⁵ In most cases the objective of the investigation was the measurement of the vibrational frequencies of the unstable species and their assignment to molecular vibrations, thereby elucidating the structure of the ion radical and the structural changes induced by the electron transfer process from or to the parent molecule. To facilitate recording the RR spectra with conventional spectrometers, decay of the RR signal is often eliminated by the application of low temperatures⁶ or steady-state conditions.^{1c} In addition to spectroscopic characterization time-resolved resonance Raman (TR³) spectroscopy can be used to measure the kinetics of intermediates in photochemical reactions and thus contribute to the elucidation of reaction mechanisms.

Kinetic information is obtained from the dependence of the intensity of a specific resonance Raman line of the short-lived species on the delay time between its creation and detection. Relatively few examples of quantitative kinetic data derived from TR³ measurements have been reported.⁷⁻¹⁰ It should be emphasized that, in some cases, the knowledge of the kinetic behavior of the transient species is essential in order to determine the nature of the unstable species, i.e., to distinguish between homogeneous and geminate radical ion pairs in electron-transfer reactions.^{8a}

In this contribution we report on investigations of the photoreactions between *trans*-stilbene and the electron-acceptors fumaronitrile (FN), 9-cyanoanthracene (CNA), and 9,10-dicyanoanthracene (DCA) in acetonitrile solution. In all cases the same transient RR spectrum is observed; however, the mechanisms for formation and decay of transients are different. The transient spectrum is assigned to the *trans*-stilbene cation radical (TS⁺), whose RR spectrum has not previously been reported. The observed RR spectrum differs significantly from the RR spectrum of the *trans*-stilbene anion radical,^{7,8} whereas the electronic absorption spectra of both ion radicals are more or less identical. Here the main advantage of transient vibrational spectroscopy over transient absorption spectroscopy with respect to the identification of short-lived intermediates in chemical reactions is clearly demonstrated: vibrational spectra are more characteristic of the structure of a molecule than electronic spectra. Special attention is paid to the decay kinetics of the *trans*-stilbene cation radical in these reactions under various experimental conditions. The kinetics support the identification of the cation radical and serve to elucidate its chemical behavior.

Experimental Section

Time-Resolved Resonance Raman Spectra. The apparatus (Figure 1) is described in detail elsewhere.¹¹ Modifications have

(1) Recent reviews are, e.g. (a) Atkinson, G. H. In "Advances in IR and Raman Spectroscopy"; Clark, R. J. H.; Hester, R. E., Eds.; Heyden: London, 1982; Vol. 9. (b) Atkinson, G. H. In "Advances in Laser Spectroscopy"; Garetz, B. A.; Lombard, J. R., Eds.; Heyden: London, 1982. (c) Hester, R. E. In "Advances in IR and Raman Spectroscopy"; Clark, R. J. H.; Hester, R. E., Eds.; Heyden: London, 1978; Vol. 4.

(2) (a) Forster, M.; Girling, R. B.; Hester, R. E. *J. Raman Spectrosc.* **1982**, *12*, 36-48. (b) Hester, R. E.; Williams, K. P. *J. Chem. Soc., Perkin Trans. 2* **1982**, 559-63. (c) Forster, M.; Hester, R. E.; Cartling, B.; Wilbrandt, R. *Biophys. J.* **1982**, *38*, 111-6. (d) Tripathi, G. N. R.; Schuler, R. H. *J. Chem. Phys.* **1982**, *76*, 2139-46. (e) Hester, R. E.; Williams, K. P. *J. Chem. Soc., Faraday Trans. 2* **1982**, *78*, 573-84. (f) Tripathi, G. N. R. *J. Chem. Phys.* **1981**, *74*, 6044-9. (g) Hester, R. E.; Williams, K. P. *J. Chem. Soc., Perkin Trans. 2* **1981**, 852-9. (h) Ernstbrunner, E. E.; Girling, R. B.; Grossmann, W. E. L.; Mayer, E.; Williams, K. P. *J. Raman Spectrosc.* **1981**, *10*, 161-8.

(3) (a) Beck, S. H.; Brus, L. E. *J. Am. Chem. Soc.* **1983**, *105*, 1106-11. (b) Rossetti, R.; Beck, S. M.; Brus, L. E. *Ibid.* **1982**, *104*, 7322-4. (c) Beck, S. M.; Brus, L. E. *Ibid.* **1982**, *104*, 4789-92. (d) Hester, R. E.; Williams, K. P. *J. Raman Spectrosc.* **1982**, *13*, 91-5. (e) Stein, P.; Ternner, J.; Spiro, T. G. *J. Phys. Chem.* **1982**, *86*, 168-70. (f) Beck, S. M.; Brus, L. E. *J. Am. Chem. Soc.* **1982**, *104*, 1805-8. (g) Forster, M.; Hester, R. E. *Chem. Phys. Lett.* **1982**, *85*, 287-92. (h) Forster, M.; Hester, R. E. *J. Chem. Soc., Faraday Trans. 2* **1981**, *77*, 1535-45. (i) Hester, R. E.; Williams, K. P. *J. Ibid.* **1981**, *77*, 541-7. (k) Williams, K. P. J.; Hester, R. E. *J. Raman Spectrosc.* **1981**, *10*, 169-72.

(4) (a) Tripathi, G. N. R.; Schuler, R. H. *J. Chem. Phys.* **1982**, *76*, 4289-90. (b) Lee, P. C.; Schmidt, K.; Gordon, S.; Meisel, D. *Chem. Phys. Lett.* **1981**, *80*, 242-7. (c) Wilbrandt, R.; Jensen, N. H.; Pagsberg, P.; Sillesen, A. H.; Hansen, K. B.; Hester, R. E. *J. Raman Spectrosc.* **1981**, 24-6. (d) Cartling, B.; Wilbrandt, R. *Biochim. Biophys. Acta* **1981**, *637*, 61-8.

(5) van Duyne, R. P. *J. Phys. C* **1977**, *5*, 259.

(6) Teraoka, J.; Ogura, T.; Kitagawa, T. *J. Am. Chem. Soc.* **1982**, *104*, 7354-6.

(7) Takahashi, C.; Maeda, S. *Chem. Phys. Lett.* **1974**, *28*, 22.

(8) (a) Hub, W.; Schneider, S.; Dörr, F.; Oxman, J. D.; Lewis, F. D. *J. Am. Chem. Soc.*, in press. (b) Hub, W.; Schneider, S.; Dörr, F.; Simpson, J. T.; Oxman, J. D.; Lewis, F. D. *J. Am. Chem. Soc.* **1982**, *104*, 2044-5. (c) Dosser, L. R.; Pallix, J. B.; Atkinson, G. H.; Wang, H. C.; Levin, G.; Szwase, M. *Chem. Phys. Lett.* **1979**, *62*, 555.

(9) (a) Jeanmaire, D. L.; van Duyne, R. P. *J. Electroanal. Chem.* **1975**, *66*, 235. (b) Ternner, J.; Campton, A.; El-Sayed, M. A. *Proc. Natl. Acad. Sci. U.S.A.* **1977**, *74*, 5212-6. (c) Friedman, J. M.; Lyons, K. B. *Nature (London)* **1980**, *284*, 570-2. (d) Shindo, H.; Hiraishi, J. *Chem. Phys. Lett.* **1981**, *80*, 238-41. (e) Tripathi, G. N. R.; Schuler, R. H. In "Time-Resolved Vibrational Spectroscopy"; Atkinson, G. H., Ed.; Heyden: London, 1983.

(10) Atkinson, G. H.; Gilmore, D. A.; Dosser, L. R.; Pallix, J. B. *J. Phys. Chem.* **1982**, *86*, 2304-10.

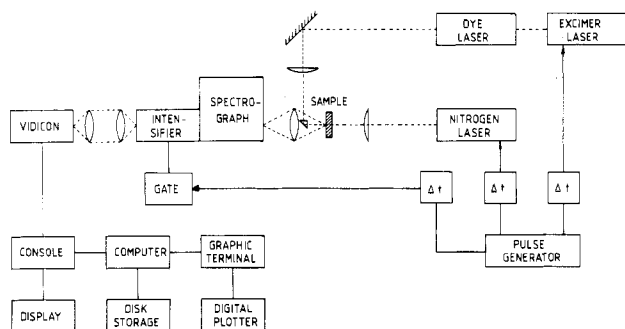


Figure 1. Block diagram of the apparatus used to measure the TR³ spectra.

been made only in the cell arrangement, which was set to 180° backscattering illumination by the RR probe laser (excimer laser pumped dye laser, 15 ns, 3 mJ/pulse). The solution flows through a 1 × 4 cm fused silica cell of 2 mm thickness in a direction perpendicular to the laser beam. The cell is connected to a reservoir in which the solution can be bubbled with nitrogen, argon, or oxygen. The flow rate is adjusted such that each laser pulse hits a fresh solution (repetition rate 5 s⁻¹). The photolysis laser beam (N₂ laser 337 nm, 5 ns, 0.5 mJ/pulse) counterpropagates the probe laser beam. The pump and probe beams are thoroughly focussed and aligned for maximum overlap in the cell. The scattered light is spectrally dispersed in a double-grating spectrograph, intensified by a gated image intensifier (EMI 9912), and focussed onto the cooled (-20 °C) vidicon of an optical multichannel analyzer (PAR OMA 1). The spectrograph is normally set to transmit a window of 650 cm⁻¹. By means of two different gratings in each half of the spectrograph the spectral window can be varied between 4540 and 500 cm⁻¹ at 500 nm. Spectra with partially overlapping spectral regions are processed by a minicomputer (MINC 11/23) to give a complete Raman spectrum. Each of the transient Raman spectra is measured with the same integrated photolysis and probe laser intensities and with a constant delay time between laser pulses. All measurements are carried out at room temperature.

TR³ Kinetic Measurements. A kinetic analysis of TR³ data for first-order reactions was given by Atkinson.¹⁰ The evaluation of the rate constant from experimental TR³ data is significantly different in the case of second order reactions as the value of the parameter cannot be determined absolutely. We will discuss in this section the dependence of the intensity of the Raman scattered light $I_T(t, \nu)$ of a transient species on its concentration $c_T(t)$. $I_T(t, \nu)$ is time dependent not only because $c_T(t)$ is changing with the delay time between the pump and the probe laser pulse but also because the optical density of the illuminated sample volume at the probe laser frequency ν_0 depends on $c_T(t)$. Therefore the probe laser intensity $I(t, \nu_0)$ cannot be considered to be constant at all delay times. In eq 1 $I_T(t, \nu)$ is given as a function of the geometrical

$$I_T(t, \nu) = AI(t, \nu_0)v_T^4\sigma_T(\nu_T, \nu_0)c_T(t)10^{c_T(t)x_T\epsilon(\nu_T)} \quad (1)$$

factor A , the probe laser intensity $I(t, \nu_0)$, the fourth power of the frequency of the scattered light ν_T for a specific RR band ν_i of the transient species ($\nu_T = \nu_0 - \nu_i$), the RR scattering cross section $\sigma_T(\nu_T, \nu_0)$, the concentration of the transient species $c_T(t)$, and a correction factor for the reabsorption of the scattered light with frequency ν_T at the distance x from the entrance window (backscattering geometry). The time dependence of $I(t, \nu_0)$ also influences the simultaneously measured intensity of the solvent Raman band $I_S(t, \nu)$ (eq 2). Obviously the RR intensity $I_T(t, \nu)$

$$I_S(t, \nu) = AI(t, \nu_0)v_S^4\sigma_S(\nu_S, \nu_0)c_S10^{c_T(t)x_S\epsilon(\nu_S)} \quad (2)$$

itself cannot be used to directly derive the kinetic data of the transient species as its quantitative relation to $c_T(t)$ is not known. The relative intensity $I_r(t, \nu)$ (eq 3a), however, depends linearly on the concentration of the transient species $c_T(t)$ under the

$$I_r(t, \nu) = \frac{I_T(t, \nu)}{I_S(t, \nu)} = \frac{v_T^4}{v_S^4\sigma_S(\nu_S, \nu_0)c_S}\sigma_T(\nu_T, \nu_0)c_T(t)10^{c_T(t)[x_T\epsilon(\nu_T) - x_S\epsilon(\nu_S)]} \quad (3a)$$

following experimental conditions: (i) ν_0 is held constant during the simultaneous measurement of the intensities $I_T(t, \nu)$ and $I_S(t, \nu)$ of a selected pair of transient and solvent Raman bands as a function of the delay time between photolysis and probe pulse and (ii) the reabsorption is the same for both scattered frequencies, i.e., $x_T\epsilon(\nu_T) \approx x_S\epsilon(\nu_S)$ (eq 3b).

$$I_r(t, \nu) \approx \frac{v_T^4\sigma_T(\nu_T, \nu_0)}{v_S^4\sigma_S(\nu_S, \nu_0)}c_T(t) \equiv Sc(t) \quad (3b)$$

The delay time dependence of $I_r(t, \nu)$ can be used to determine the order of the chemical reactions of the transient species and the rate constant in special cases. The following brief discussion of this possibility only deals with first- and second-order reactions as these are most important in photochemically induced electron-transfer reactions. The significance of $I_r(t, \nu)$ is different for the two types of reactions. For first-order reactions the slope of the plot of $\log(I_r(t, \nu))$ vs. time gives directly the exact value of the rate constant, although the concentration of the transient species cannot be determined from the intercept as the scattering cross section for the transient resonance Raman band in the term S in eq 3b is normally not known. For second-order reactions of the type $A + B \rightarrow C + D$ with equal concentrations of A and B the plot of $I_r(t, \nu)^{-1}$ vs. time should be a straight line with the slope k/S (eq 3b). Here neither the rate constant nor the concentration can be determined. This is also the case in the general type of second-order reactions with nonequal concentrations of A and B as well as for higher-order reactions.

The logarithm of the ratio of the solvent Raman band ($\nu_s = \nu_0 - \nu_i$) intensity of the unphotolyzed solution $I_S'(v)$ and the value $I_S(t, \nu)$ in the photolyzed solution (eq 4) is an internal measure

$$R = \log \frac{I_S'}{I_S(t, \nu)} = [x_S\epsilon(\nu_S) + x_0\epsilon(\nu_0)]c_T(t) \quad (4)$$

of the transient absorption¹⁰ in the solution at the time t after the photolysis pulse and thus has the same significance as conventional transient absorption data for the evaluation of kinetic data. The difference between the two kinds of information buried in eq 3 and eq 4 is that $I_r(t, \nu)$ only depends on a single transient species whereas the quantity R reflects the absorption properties of the solution within the bandwidth of the solvent Raman band, which can be attributed to more than one transient species. Under such conditions it could be advantageous to follow the kinetics by means of $I_r(t, \nu)$ rather than by means of R .

The kinetics of the *trans*-stilbene cation radical is measured by the following procedure: A spectral window is chosen such that at least one solvent band and one TR³ band of comparable intensity are observed simultaneously. For a given delay time between the pump and the probe laser pulse the TR³ spectrum is accumulated over 500–1500 pulse pairs. Then the spontaneous Raman spectrum of the unphotolyzed solution is accumulated until the solvent bands are completely compensated in the difference spectrum. This is normally achieved with fewer pulses than in the TR³ case since the probe laser light is not partially absorbed by the transient species. $I_r(t, \nu)$ is determined by dividing the integrated intensity of the transient band in the difference spectrum by the integrated intensity of the solvent band in the second spectrum. Since the bands of the transient species partially overlap other bands, it is not possible to simply take the ratios of the intensities in the TR³ spectrum. The $I_r(t, \nu)$ data are determined at different delay times and are analyzed by means of least-square fit routines assuming both pure first- and pure second-order rate laws. The resulting χ^2 values¹² were used to decide upon the actual

(11) Dörr, F.; Hub, W.; Schneider, S. *J. Mol. Struct.* **1980**, *60*, 233–8.

(12) Bevington, P. R. "Data Reduction and Error Analysis for the Physical Sciences", McGraw-Hill: New York, 1969.

TABLE I: Resonance Raman Frequencies (cm^{-1}) of the *trans*-Stilbene Cation Radical and Raman Frequencies of *trans*-Stilbene in Acetonitrile Solution (Excitation Wavelength 480 nm)

TS*		TS
with FN	with DCA	
1605 vs	1605 vs	1638 vs 1595 s 1488 m 1445 m
1342 m	1345 w	1337 s
1281 s	1285 s	1188 s 1180 s
988 m	989 m	992 vs
858 m	859 m	866 m
628 m	628 w	616 m

reaction order. All the $I_r(t, \nu)$ values reported here are taken with the same pair of transient and solvent band ($1605/2253 \text{ cm}^{-1}$) and with the same probe laser wavelength (480.0 nm). Therefore the factor S in eq 3b is constant throughout the measurements and the values of k/S in different solutions reflect the changes in the relative rate constants.

Resonance Raman Excitation Profiles. For a given pair of transient and solvent Raman bands the value of $I_r(t, \nu)$ is a linear function of the RR scattering cross section of the transient band if the following conditions hold (eq 3b): (i) the delay time between pump and probe laser pulse must be constant and (ii) the solvent Raman band intensity should not significantly vary with the probe laser frequency ν_0 . This condition is normally obeyed if $\nu_0 \ll \nu_e$, where ν_e is the frequency of the lowest electronic transition in the solvent molecule. The RR excitation spectrum (plot of $I_r(t, \nu)$ vs. ν_0) can be compared to the electronic absorption spectrum of the molecule studied, thereby providing further support for its identification. $I_r(\nu=\nu_0)$ (eq 3) has been measured at a constant delay time as a function of ν_0 and the values corrected for the sensitivity of the detection system, the extinction of the solution at ν_S and ν_T , and for the factor ν_S^4/ν_T^4 (eq 3b).

Chemicals. *trans*-Stilbene (Aldrich) was purified by recrystallization from ethanol and benzene. Fumaronitrile (Aldrich) was recrystallized from benzene, then vacuum sublimed. 9-Cyanoanthracene (Merck) and 9,10-dicyanoanthracene (Merck) were recrystallized from ethanol. Acetonitrile (Aldrich spectrograde) was refluxed over calcium hydride and distilled through a 1-m column (bp 86.8°C). High-purity nitrogen, argon, or oxygen (Messer Griesheim) were used to saturate the solutions by bubbling them before and during the measurements.

Quantum Yields. Acetonitrile solutions of TS with FN or DCA were purged with nitrogen or oxygen prior to irradiation on a merry-go-round apparatus with monochromatic 313- (FN) or 365-nm (DCA) light provided by the filtered output of a Hanovia 450-W medium-pressure mercury lamp in a water-cooled Pyrex lamp well. Light intensities were determined with *trans*-stilbene (313 nm)¹³ or Amberchrom 540 (365 nm)¹⁴ actinometers. Irradiated solutions were analyzed for product formation at low (<10%) conversions of TS to CS or benzaldehyde by using a calibrated 6 ft \times 1/8 in. column containing 5% SF-96 on Chromasorb G with a Varian 3700 flame ionization gas chromatograph.

Results

Time-Resolved Resonance Raman Spectroscopy of *trans*-Stilbene and Fumaronitrile. The spontaneous Raman spectrum of a solution of 0.05 M TS and 0.2 M FN in nitrogen-saturated acetonitrile is shown in Figure 2b. The frequencies are due to TS (1638, 1595, 1188, 992 cm^{-1}) and acetonitrile (2253, 1372, 917 cm^{-1}) (Table I). Additional frequencies appear at 1605, 1342, 1281, 988, 858, and 628 cm^{-1} if the solution is photolyzed 60 ns before the spectrum is measured (Figure 2a). In the difference

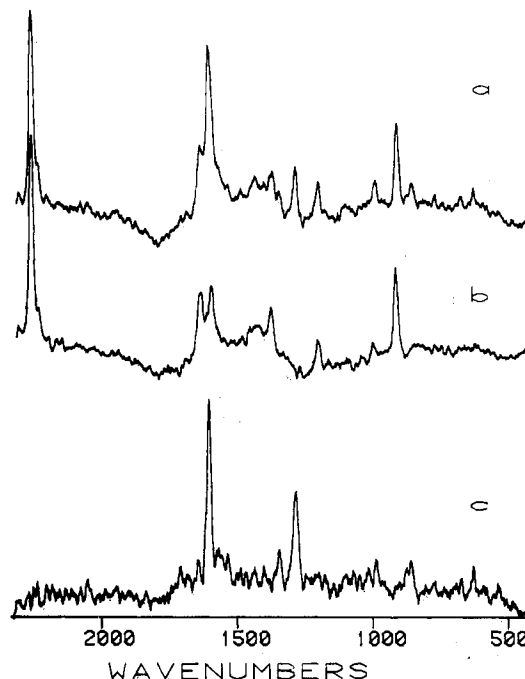


Figure 2. (a) TR³ spectrum of a solution of 0.05 M *trans*-stilbene and 0.2 M fumaronitrile in nitrogen-saturated acetonitrile. The spectrum is taken 60 ns after the photolysis pulse with a probe wavelength of 480.0 nm. (b) Raman spectrum of the same solution without photolysis. (c) Difference spectrum a - b containing only transient bands.

TABLE II: Second-Order Rate Constants k/S (Eq 3) and Half-Lives from Time-Dependent RR Band Intensities (1605 cm^{-1}) Normalized to Solvent Band Intensity (2253 cm^{-1})^a

electron acceptor	O ₂	$10^{-6} k/S$, au/s	$t_{1/2}$, ns
fumaronitrile			
0.05 M	-	0.9	1100
0.20 M	-	1.7	440
0.05 M	+	5.6	180
0.20 M	+	5.6	80
dicyanoanthracene			
2×10^{-4} M	-	4.4	120
2×10^{-4} M	+	7.0	110

^a Solutions contained 0.05 M *trans*-stilbene in acetonitrile at room temperature.

spectrum (Figure 2c), which only contains bands of transient species, both the intense solvent band at 2253 cm^{-1} and the TS bands are compensated. If we assume that a reduction of the TS band intensity of $\approx 5\%$ due to the formation of the transient species should result in obvious overcompensation of the TS bands when the solvent bands are fully compensated in the difference spectrum then the absence of overcompensation allows an estimate of 0.002 M for the upper limit for the concentration of the transient species. All transient bands are due to a single species as their intensities show the same decay after the photolysis pulse (monitored up to 600 ns for the two intense (Figure 3) and up to 200 ns for the weaker bands).

The decay of the band at 1605 cm^{-1} (intensity normalized to the 2253 cm^{-1} solvent band intensity) in nitrogen-saturated solutions of *trans*-stilbene (0.05 M) and fumaronitrile depends on the FN concentration (Figure 3a): The decay rate is $k/S = 9 \times 10^5 \text{ au/s}$ for 0.05 M FN and $k/S = 1.7 \times 10^6 \text{ au/s}$ for 0.2 M FN (Table II). The χ^2 value³³ for pure first- and pure second-order fits (0.02 and 0.04, respectively) are not very significant due to the short observation time with respect to the observed half-life. The initial intensity of the TR³ band is 1.4 times higher with the lower FN concentration as with the higher concentration.

When the solutions are saturated with oxygen the second-order rate constant is higher and independent of the FN concentration ($k/S = 5.6 \times 10^6 \text{ au/s}$) (Table II). If we assume a maximum

(13) Lewis, F. D.; Johnson, D. E. *J. Photochem.* **1977**, *7*, 421-3.

(14) Heller, H. G.; Langan, C. R. *J. Chem. Soc., Perkin Trans. 1* **1981**, 341.

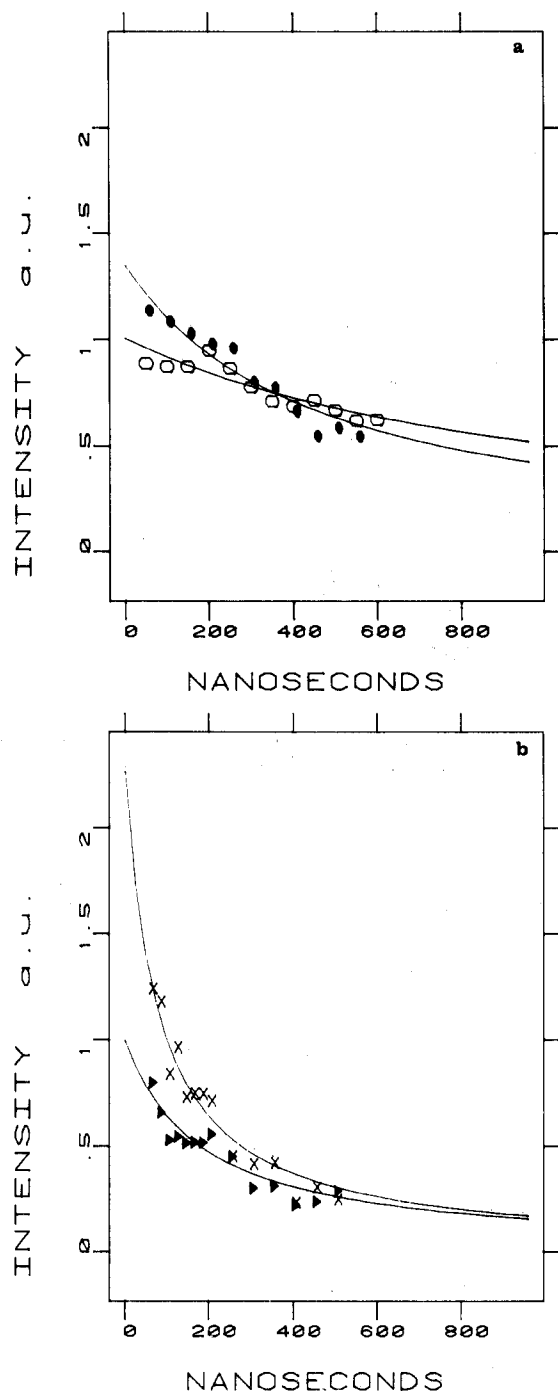


Figure 3. (a) Decay of TS^+ signal intensity $I_r(t)$ (1605 cm^{-1}) in nitrogen-saturated solution of 0.05 M *trans*-stilbene and 0.05 M (●) or 0.2 M (○) fumaronitrile. (b) Same as in (a) but in oxygen-saturated solutions: 0.05 M FN (▼), 0.2 M FN (×). Second-order fits are drawn as a full line.

concentration of the transient species of 10^{-3} M (see above), then the minimum rate constant is $6 \times 10^9\text{ M}^{-1}\text{ s}^{-1}$ which points to a nearly diffusion-controlled process.

Time-Resolved Resonance Raman Spectroscopy of *trans*-Stilbene and Cyanoanthracene. The TR^3 spectra of solutions of $2 \times 10^{-4}\text{ M}$ DCA with 0.05 M TS were measured in aerated and argon-saturated acetonitrile between 60 and 900 ns after the photolysis pulse. Figure 4 shows the transient spectra obtained as the difference between the spectrum of the photolyzed solution (80 ns) and the spontaneous Raman spectrum ($\lambda_0 = 485.3\text{ nm}$) of the solution without photolysis. The criterion for the subtraction was again the compensation of the most intense solvent band at 2253 cm^{-1} , which also compensated completely the other solvent bands and the bands from the TS starting material. According

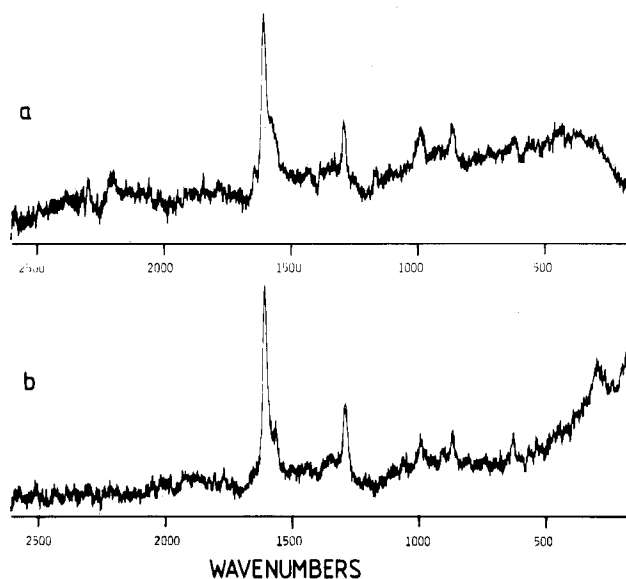


Figure 4. TR^3 spectrum of the *trans*-stilbene cation radical in solutions of 0.05 M *trans*-stilbene and $4 \times 10^{-4}\text{ M}$ 9,10-dicyanoanthracene 80 ns after the photolysis. The solutions are bubbled with nitrogen (a) or air (b).

to the considerations outlined in the section dealing with TS-FN results, the concentration of the transient species must be $<0.002\text{ M}$. In fact it is limited by the concentration of DCA ($4 \times 10^{-4}\text{ M}$).

In both spectra (Figure 4, a and b) bands at 1605 , 1345 , 1285 , 989 , 859 , and 628 cm^{-1} are observed which are the same as in the TS-FN solutions (Table I). In deoxygenated solutions additional weak bands at 1650 and 1162 cm^{-1} appear (Figure 4a).

The same TR^3 spectrum as in Figure 4a is obtained in the reaction of TS with CNA, but here the intensity of the transient RR bands at a given delay time is much less than in the case of DCA. This may be due in part to less efficient fluorescence quenching by 0.05 M TS for CNA (86% quenching) vs. DCA (94% quenching).¹⁵ Also with CNA a significant emission background is observed around 520 nm at short delay times.

The yield and the decay of the transient species are dependent upon the oxygen concentration. In oxygen-saturated solutions the decay rate is increased from $k/S = 4.4 \times 10^6\text{ au/s}$ (argon) to $k/S = 7 \times 10^6\text{ au/s}$ (Figure 5), whereas the initial yield of TS^+ is reduced to about 70% of the value in argon-saturated solutions. A similar reduction of the initial yield and increase in the decay rate were reported by Spada and Foote.¹⁶

The excitation profile for the band at 1605 cm^{-1} exhibits a maximum around 470 nm (Figure 6), in excellent agreement with the literature values¹⁷⁻²⁰ for the visible absorption band of the *trans*-stilbene cation radical.

Stilbene Isomerization and Oxidation. Irradiation (313 or 365 nm) of TS (0.05 M) and FN (0.1 M) in oxygenated or deoxygenated benzene or acetonitrile solutions results in the formation of CS and maleonitrile in a ratio of ca. $15/1$.^{22a} Also formed in oxygenated acetonitrile solution are benzaldehyde and lesser amounts of benzil and stilbene oxide. Quantum yields for product formation are summarized in Table III. Quantum yields for CS formation decrease with increasing FN concentration as shown in Figure 7. Assumption of simple exciplex quenching kinetics (eq 5) allows values of the limiting quantum yield for CS formation

$$\Phi_{CS}^{-1} = (\Phi_{CS}^0)^{-1}(1 + k_q\tau[\text{FN}]) \quad (5)$$

in the absence of exciplex quenching (Φ_{CS}^0) and the quenching

- (15) Eriksen, J.; Foote, C. S. *J. Phys. Chem.* **1978**, *82*, 2659-62.
 (16) Spada, L. T.; Foote, C. S. *J. Am. Chem. Soc.* **1980**, *102*, 391-3.
 (17) Gooden, R.; Brauman, J. I. *J. Am. Chem. Soc.* **1982**, *104*, 1483-6.
 (18) Shida, T.; Hamill, W. J. *J. Chem. Phys.* **1966**, *44*, 2375.
 (19) Torikai, A.; Kato, H.; Kuri, Z.-I. *J. Polym. Sci.* **1976**, *14*, 1065-71.
 (20) Rodgers, M. A. J. *Faraday Soc. Trans.* **1971**, *67*, 1029.

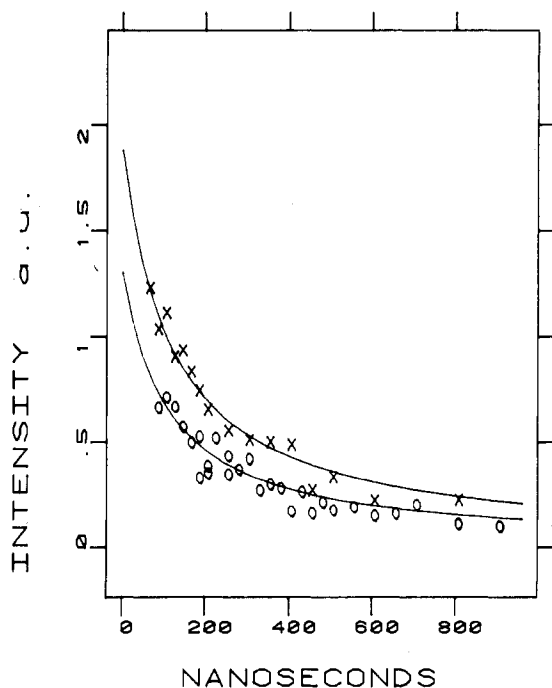


Figure 5. Decay of the TS^+ signal intensity $I_r(t)$ (1605 cm^{-1}) of a solution of 0.05 M *trans*-stilbene and $4 \times 10^{-4}\text{ M}$ 9,10-dicyanoanthracene saturated with argon (X) or oxygen (O). Second-order fits are drawn as a full line.

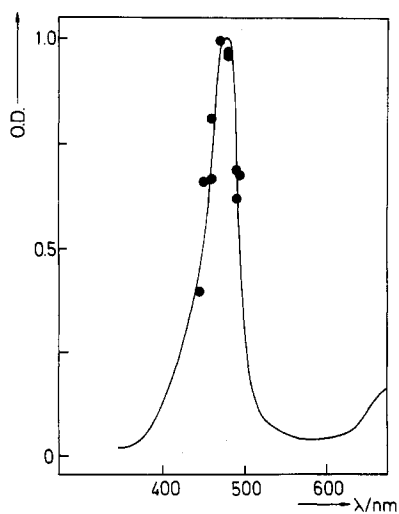


Figure 6. Excitation profile of the 1605-cm^{-1} band of TS^+ (●) and its absorption spectrum.¹⁷

TABLE III: Quantum Yields for *cis*-Stilbene and Benzaldehyde Formation

electron acceptor	solvent	O ₂	Φ_{CS}^a	Φ_{BA}
fumaronitrile				
0.20 M	C ₆ H ₆	-	0.11 (0.12) ^b	
0.20 M	C ₆ H ₆	+	0.17 (0.26) ^b	<0.001
0.10 M	CH ₃ CN	-	0.22 (0.56) ^c	
0.10 M	CH ₃ CN	+	0.31 ^c	0.002
dicyanoanthracene				
$3 \times 10^{-4}\text{ M}$	C ₆ H ₆	-	0.011 ^d	
$3 \times 10^{-4}\text{ M}$	C ₆ H ₆	+	0.032 ^d	<0.001
$3 \times 10^{-4}\text{ M}$	CH ₃ CN	-	0.002 ^d	
$3 \times 10^{-4}\text{ M}$	CH ₃ CN	+	0.013 ^d	0.060

^a Data for 0.05 M TS except where indicated. Values in parentheses in the limit of low FN concentration (Figure 7) or high oxygen concentration. ^b Data from Lewis and Simpson²² for 0.1 M TS, 365-nm irradiation of the ground-state complex. ^c Data for 313-nm irradiation of TS corrected for incomplete quenching of TS by FN. ^d Data for 365-nm irradiation of DCA.

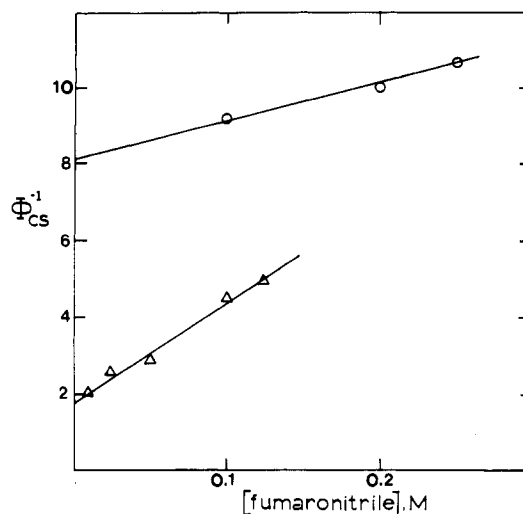
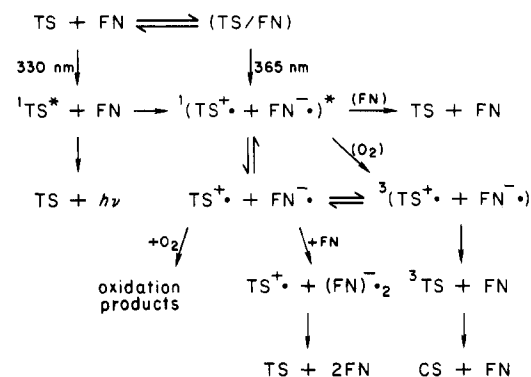


Figure 7. Fumaronitrile concentration dependence of the quantum yield for *cis*-stilbene formation in deoxygenated benzene (O) and acetonitrile (Δ) solution.

Scheme I. Mechanism of Photoreaction of *trans*-Stilbene with Fumaronitrile in Acetonitrile Solution



constant ($k_q\tau$) to be obtained from the intercept and slope/intercept ratios of Figure 7. Values of Φ_{CS}^0 are reported in Table III. Values of $k_q\tau = 1.3$ and 15 M^{-1} are obtained for benzene and acetonitrile solution, respectively. Irradiation (365 nm) of TS (0.05 M) and DCA ($3 \times 10^{-4}\text{ M}$) in deoxygenated benzene or acetonitrile solution results in highly inefficient formation of CS. Under the reaction conditions all of the incident light is absorbed by DCA and >95% of singlet DCA is quenched by TS. Irradiation of oxygenated solutions results in an increase in the quantum yield for CS formation and, in acetonitrile solution, the formation of benzaldehyde and lesser amounts of benzil and stilbene oxide. Quantum yields for CS and benzaldehyde formation are summarized in Table III. The total quantum yield for product formation in oxygenated acetonitrile solution is 0.1 ± 0.02 . A higher value (0.5) was reported by Eriksen and Foote²¹ based on extrapolation of low concentration data for 405-nm irradiation. Differences in TS concentration and excitation wavelength may account for the discrepancy in the quantum yields.

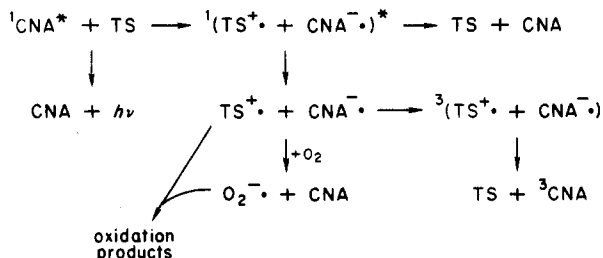
Discussion

Photochemical Reaction of trans-Stilbene with Fumaronitrile. Previous investigations of this reaction by several groups^{22,23,29,31} are consistent with the mechanism outlined in Scheme I. Excitation of either TS (313 nm) or the weak ($K_{eq} \sim 0.5$)²³ TS-FN charge-transfer complex (365 nm) in nonpolar solvent results in the formation of a weakly fluorescent exciplex ($\Phi_f = 0.013$, $\tau = 13\text{ ns}$)^{22a,23} with an emission maximum corresponding to an energy

(21) Eriksen, J.; Foote, C. S. *J. Am. Chem. Soc.* **1980**, *102*, 6083-8.

(22) (a) Lewis, F. D.; Simpson, J. T. *J. Phys. Chem.* **1979**, *3*, 2015-9. (b) Lewis, F. D. *Acc. Chem. Res.* **1979**, *12*, 152.

(23) Adams, B. K.; Cherry, W. R. *J. Am. Chem. Soc.* **1981**, *103*, 6904-7.

Scheme II. Mechanism of Reaction of Ground-State *trans*-Stilbene with Singlet Cyanoanthracenes in Acetonitrile Solution

of 2.34 eV. The major product derived from the singlet exciplex is *cis*-stilbene (CS), which is thought to be formed via exciplex intersystem crossing followed by decay of the triplet exciplex to yield the low-energy triplet state of TS (2.12 eV),²⁶ which yields CS with a reported quantum yield of 0.55²⁷. The low yield of isomerized FN indicates either that its higher energy triplet state (2.55 eV)⁴¹ is not populated or is populated but transfers its energy to TS prior to diffusion or isomerization.

The quantum yield for CS formation from the TS–FN exciplex in benzene solution decreases slightly with increasing FN concentration (Figure 7). The value in the limit of low FN concentration is 0.12, providing a value for the quantum yield for exciplex intersystem crossing of 0.22. The rate constant for exciplex quenching by ground-state FN obtained from the slope/intercept ratio of Figure 7 ($k_q\tau = 1.3 \text{ M}^{-1}$) by using eq 5 and the measured value of τ is $k_q = 1.0 \times 10^8 \text{ M}^{-1} \text{ s}^{-1}$. The quantum yield for CS formation from the singlet exciplex increases with increasing oxygen concentration to a limiting value of 0.25 (Table III), as a result of oxygen enhancement of intersystem crossing. No photooxidation of TS is observed in benzene solution.

In polar solvents excitation of TS and FN results in the formation of a nonfluorescent singlet radical ion pair. In the limit of low FN concentration, the quantum yield for CS formation is 0.56 (Table III), indicating that all of the initially formed geminate radical ion pairs ultimately yield triplet TS. Quenching of CS formation by ground-state FN (Figure 7, $k_q\tau = 15 \text{ M}^{-1}$) is more efficient in polar vs. nonpolar solvent, indicating either an increase in k_q or the lifetime of the precursor of triplet TS. In the presence of oxygen the quantum yield for CS formation increases and benzaldehyde, the major photooxidation product from TS, is formed in low yield. Increased isomerization presumably results from oxygen-catalyzed intersystem crossing, which shortens the lifetime of the singlet geminate radical ion pair and thus decreases the extent of quenching by ground-state FN. The low quantum yield for benzaldehyde formation indicates that diffusion of the geminate radical ion pair to form homogeneous radical ions is highly inefficient, in agreement with a previous conclusion based on the low CIDNP signal intensity for CS formed in this reaction³¹ and with our TR³ results. Thus the predominant pathway leading to triplet TS is intersystem crossing of the geminate radical ion pair and not homogeneous radical ion pair recombination. A lower limit for the lifetime of the geminate radical ion pair of 0.5 ns can be estimated from the value of $k_q\tau$ obtained from Figure 7 and the calculated rate of diffusion in acetonitrile solution ($3 \times 10^{10} \text{ M}^{-1} \text{ s}^{-1}$).²⁴

Photochemical Reaction of *trans*-Stilbene with Dicyanoanthracene. Previous investigations of this reaction by Foote and co-workers^{15,16,21} are consistent with the mechanism outlined in Scheme II. Quenching of singlet DCA by TS in benzene or acetonitrile solution results in neither exciplex fluorescence nor

efficient formation of CS (Table III). The formation of radical ions in polar solvent was indicated by the observation of TS^{•+} by transient absorption spectroscopy (470 nm)¹⁶ and of DCA^{•-} by ESR.²⁸ The low quantum yields for CS formation indicate either that the triplet exciplex ($E_{\text{ex}} \sim 2.3 \text{ eV}$)²⁵ is formed inefficiently or that, when formed, it yields triplet DCA ($E_{\text{T}} \sim 1.8 \text{ eV}$) rather than triplet TS ($E_{\text{T}} \sim 2.12 \text{ eV}$). The increase in the quantum yield for CS formation in the presence of oxygen may result from the production of triplet DCA upon quenching of singlet DCA by oxygen,⁴⁴ followed by triplet energy transfer from DCA to TS. If we assume diffusion-controlled quenching of DCA by TS (0.05 M) and oxygen ($2 \times 10^{-3} \text{ M}$), the efficiency of triplet DCA formation is ca. 0.05, sufficiently large to account for the increased quantum yields for CS formation in the presence of oxygen. The larger quantum yield for CS formation in degassed benzene vs. acetonitrile solution indicates that CS is not formed via isomerization of free CS^{•+}, as suggested by Eriksen and Foote.

Benzaldehyde is the major product observed upon irradiation of DCA and TS in oxygenated acetonitrile solution. The absence of benzaldehyde formation in benzene solution supports its formation via reactions of homogeneous radical ions with oxygen (Scheme II). The substantially higher quantum yield for benzaldehyde formation from the DCA–TS vs. TS–FN system indicates that cage escape of the initially formed geminate radical ion pair is much more efficient for the former system, in accord with our TR³ results.

Nature of the Transient Species. Since we find identical TR³ spectra in the reactions of TS with FN, DCA, and CNA, the transient species must be related to TS. Based on previous photochemical investigations of these reactions two intermediates derived from *trans*-stilbene need to be considered: The triplet-state molecule (³TS) and the cation radical (TS^{•+}). The RR spectrum of each of these possible intermediates should be significantly different than the Raman spectrum of *trans*-stilbene as a result of the absence of one electron in the cation radical and of the twisted structure in the excited triplet state.²⁷ As the RR spectra of neither species is known in the literature, the identification of the transient species is based on a discussion of (i) the RR spectrum, (ii) the excitation profile, and (iii) the decay kinetics measured via the time dependence of the RR band intensity.

The most striking differences between the Raman spectra of the transient species and normal TS are the disappearance of the central C=C stretching frequency at 1638 cm⁻¹ and of the phenyl-C stretching frequency at 1188 cm⁻¹ and the appearance of a new strong band at 1285 cm⁻¹. These observations are in accord with the changes expected as a result of the loss of an electron when TS is transformed to its cation radical: Weakening of the central double bond should cause a substantial shift of the C=C stretching mode to lower frequency. The strong band at 1285 cm⁻¹ may correspond to the stretching vibration of this bond in the cation radical. Similar shifts between neutral olefins and their radical cations have been reported.³⁰ This band could also contain a contribution from the phenyl-C stretching mode which should be shifted to higher frequencies.³⁸ The frequencies which are attributed to vibrations located in the phenyl rings (1605, 988, 860, and 628 cm⁻¹) remain close to the values for the same modes in the neutral molecule (Table I). Evidently, the bond lengths in the phenyl rings are not much affected by the electron loss. The RR spectrum of the transient species differs substantially from that of the anion radical of *trans*-stilbene^{7,8} wherein the C=C stretching frequencies are shifted to 1577 and 1553 cm⁻¹, the phenyl-C stretching frequency is located at 1251 cm⁻¹, and the ring modes below 1000 cm⁻¹ are found at 978, 848, and 624 cm⁻¹. The high intensity of the 1605-cm⁻¹ band and the 1285-cm⁻¹ band of the transient species suggests that the assigned stretching modes provide the highest contribution to the Franck–Condon factors

(24) Murov, S. "Handbook of Photochemistry"; Marcel Dekker: New York, 1973.

(25) Schulten, K.; Staerk, H.; Weller, A.; Werner, H.-J.; Nickel, B. Z. Phys. Chem. (Frankfurt am Main) 1976, 101, 371–82.

(26) Saltiel, J.; D'Agostino, J.; Megarity, E. D.; Metts, L.; Neuberger, K. R.; Wrighton, M.; Zafiriou, O. C. Org. Photochem. 1973, 3, 1.

(27) Saltiel, J.; Chang, D. W. L.; Megarity, E. D.; Rousseau, A. D.; Shannon, P. T.; Thomas, B.; Uriarte, A. K. Pure Appl. Chem. 1975, 41, 559–79.

(28) Schaap, A. P.; Zaklika, K. A.; Kaskar, B.; Fung, L. W.-M. J. Am. Chem. Soc. 1980, 102, 389–91.

(29) (a) Arnold, D. R.; Wong, P. C. J. Am. Chem. Soc. 1979, 101, 1894–5. (b) Bargon, J. J. Am. Chem. Soc. 1977, 99, 8350–1.

(30) Mollere, P. D.; Houk, K. N.; Bomse, D. S.; Morton, T. H. J. Am. Chem. Soc. 1976, 98, 4732–6.

in the electronic transition of the transient species around 480 nm. Frequency shifts similar to the one observed would also be expected for the triplet state of *trans*-stilbene. Therefore without the knowledge of the RR frequencies of either the triplet or cation radical and without the help of model calculations it is not possible to identify the transient species on the basis of the observed RR spectrum alone.

In benzene solution ³TS absorbs around 360 ($\epsilon = 800 \text{ M}^{-1} \text{ cm}^{-1}$) and 420 nm.³⁷ The cation radical has a visible absorption band around 470 nm. The excellent agreement between the RR excitation profile (Figure 6) and the electronic absorption band of TS⁺ strongly supports the identification of the *trans*-stilbene cation radical as the transient species.

The additional peak around 430 nm which appears in the transient absorption spectrum of TS⁺ with CNA as sensitizer¹⁶ must therefore be due to a different molecular species, e.g., the ³CNA, which absorbs in this region.³² The emission background in the TR³ measurements at short delay times can be explained by fluorescence of unquenched ¹CNA* molecules³⁹ or of the CNA-TS exciplex. The fact that an emission is not observed with DCA as sensitizer may be due to more efficient quenching of DCA vs. CNA by 0.05 M TS or the absence of fluorescence from the DCA-TS exciplex. So that the transient species can be identified by means of time-dependent measurements several possibilities must be considered: (i) ³TS has a lifetime of 120 ns in benzene solution.^{27,37a} If we assume that its lifetime in acetonitrile is roughly the same then it becomes clear that the transient species cannot be ³TS, as the observed transient lifetimes are much longer (Table II). (ii) Geminate radical ion pairs decay in polar solvents according to a first-order rate law with half-lives of several nanoseconds or less.³⁵ As the observed decays are much slower (Table II) it follows that TS⁺ as part of the geminate radical ion pair is not the observed transient species. (iii) Triplet radical ion pairs can be formed by intersystem crossing from the singlet radical ion pairs and are most likely the precursor of the *cis*-stilbene.^{27,31} The free energies of the radical ion pairs are well above those of the triplet states of the corresponding electron-donor and -acceptor molecules.³⁴ Therefore the lifetime of the triplet radical ion pairs is expected to be on the order of nanoseconds. This means that also TS⁺ as part of the triplet radical ion pair can be ruled out as the transient species. (iv) Solvated radical ion pairs are known to undergo homogeneous recombination within 1 ns. Thus solvated TS⁺ is the only species with a predicted lifetime consistent with our observations for the transient species. In summary, the transient Raman spectrum, Raman excitation spectrum, and transient decay kinetics are uniquely consistent with the identification of the transient species as solvated TS⁺.

Additional TR³ Frequencies. We tentatively assign the additionally observed frequencies at 2211, 1650, and 1162 cm⁻¹, which appear only in deoxygenated solutions of TS and DCA, to the DCA⁻ molecule. Its transient absorption spectrum ($\lambda_{\text{max}} = 480 \text{ nm}$) is still observable 1 μs after the photolysis pulse.¹⁶ The rather low intensity of its RR spectrum may come from a lower extinction coefficient and/or RR scattering cross section than that of TS⁺ at the probe laser wavelength. The band at 2211 cm⁻¹ corresponds to the C \equiv N stretching vibration. The C \equiv N bond order is partially lowered by the addition of the electron into an antibonding orbital of the DCA molecule. A shift to lower frequencies of C \equiv N stretching vibrations in aromatic nitriles upon one-electron reduction is known to depend on the amount of participation of this bond in the conjugation of the carbon skeleton.³⁶ As the shift here is relatively small, the CN group

in DCA might be only weakly coupled to the conjugated π -system, which also would explain its rather low RR intensity.

The absence of any RR frequencies assigned to FN⁻ results from the small extinction coefficient ($\lambda_{\text{max}} = 380 \text{ nm}$) of this molecule at the probe laser wavelength.⁴⁰ The same argument applies for the failure to observe the dimer anion radical (FN)₂⁻. Typical RR frequencies of dimer radical ions are found between 100 and 200 cm⁻¹,³³ which is out of the range of our measurements.

Reactivity of the *trans*-Stilbene Cation Radical. All TS⁺·TR³ decay curves fit reasonably well to a second-order rate law for a reaction $A + B \rightarrow C + D$ with equal concentrations of A and B. This corresponds to the homogeneous recombination of the solvated radical cations and anions. The deviation from second order in the case of nitrogen-saturated TS-FN solutions is due to the comparatively short observation time (600 ns) with respect to the apparent half-life (Table II).

In deoxygenated solutions of TS and FN the decay rate of TS⁺ increases with increasing FN concentration (Table II). This is indicative of a second decay pathway for solvated TS⁺, in addition to homogeneous recombination with FN⁻. By analogy to the results of our investigations of TS/amine exciplexes we propose that FN⁻ may react with neutral FN to yield the fumaronitrile dimer anion radical (FN)₂⁻, which undergoes more rapid homogeneous recombination with TS⁺ than does FN⁻. The formation of (FN)₂⁻ has previously been proposed to account for a shift in the absorption band of FN⁻ from 450 to 980 nm upon reaction with FN under pulse radiolysis conditions. Presumably, both homogeneous recombination of TS⁺ and (FN)₂⁻ and quenching of the geminate radical ion pair by FN result in the formation of a triplex with a free energy lower than that of ³TS, thus explaining the quenching of CS formation by FN (Figure 7).

The decay rate of TS⁺ is markedly faster in oxygenated vs. deoxygenated solutions of TS and FN (Table II). The observation of benzaldehyde formation with a quantum yield comparable to that estimated for the formation of solvated TS⁺ (ca. 0.002) indicates that reaction of TS⁺ with O₂⁻ occurs with a rate constant greater than that for homogeneous recombination of TS⁺ with FN⁻. The addition of oxygen also apparently enhances the initial yield of TS⁺ obtained with high vs. low FN concentrations (Figure 3, a and b). This observation is consistent with the observed oxygen enhancement of CS formation (Table III). Oxygen-catalyzed intersystem crossing will shorten the lifetime of the singlet geminate radical ion pair thereby decreasing the efficiency of its quenching by ground-state FN. Diffusion of the triplet geminate radical ion pair to yield solvated TS⁺ in competition with formation of ³TS (Scheme I) is supported by both the increase in the initial yield of solvated TS⁺ in the presence of oxygen and by the slow rate constant for homogeneous recombination of TS⁺ and FN⁻ in the absence of oxygen.

The decay rate of TS⁺ in deoxygenated solutions is substantially faster for recombination with DCA⁻ than with FN⁻. In both cases homogeneous recombination should yield triplet and singlet geminate radical ion pairs in a 3:1 spin ratio. In both cases, locally excited triplets (TS or DCA) lie below the ion pair state. The factors which govern cage escape vs. decay of triplet exciplexes have not been elucidated; however, decay processes would be expected to be dependent upon (inter alia) energy gaps and spin-spin interactions.⁴³ The decay rates for TS⁺ in oxygenated

(31) Roth, H. D.; Schilling, M. L. M. *J. Am. Chem. Soc.* **1980**, *102*, 4303-10.

(32) Manring, L. E.; Gu, C.-I.; Foote, C. S. *J. Phys. Chem.* **1983**, *87*, 40-4.

(33) Forster, M.; Gurling, R. B.; Hester, R. E. *J. Raman Spectrosc.* **1982**, *12*, 36.

(34) The ΔG° values for the radical ion pairs are 2.7 eV (TS-FN),³¹ 2.2 eV (TS-DCA), and 2.9 eV (TS-CNA). The triplet energies are 2.1 eV (³TS),²⁶ 2.55 eV (³FN),⁴¹ 1.82 eV (³CNA),⁴² and $\sim 1.8 \text{ eV}$ (³DCA).

(35) Michel-Beyerle, M. E.; Haberkorn, R.; Bube, W.; Steffens, E.; Schröder, H.; Neusser, H. J.; Schlag, E. W.; Seidlitz, H. *Chem. Phys.* **1976**, *17*, 139.

(36) (a) Bozio, R.; Zanon, I.; Girlando, A.; Pecile, C. *J. Chem. Soc., Faraday Trans. 2* **1978**, *74*, 235-48. (b) Jeanmaire, D. L.; Suchanski, M. R.; van Duyne, R. P. *J. Am. Chem. Soc.* **1975**, *97*, 1699-707. (c) Juchnowski, I. N.; Binev, I. G. *Chem. Phys. Lett.* **1971**, *12*, 40-3.

(37) (a) Dainton, F.; Robinson, E. A.; Salmon, G. A. *J. Phys. Chem.* **1972**, *76*, 3897-904. (b) Herkstroeter, W. G.; McClure, D. S. *J. Am. Chem. Soc.* **1968**, *90*, 4522. (c) Heinrich, G.; Blume, H.; Schulte-Frohlinde, D. *Tetrahedron Lett.* **1968**, 4693.

(38) Similar shifts have been reported for the tolyl radical (Wattmann-Grajcar, L. *J. Chim. Phys.* **1969**, *66*, 1023-40) and for the excited singlet state of *trans*-stilbene (Dyck, R. H.; McClure, D. S. *J. Chem. Phys.* **1962**, *36*, 2326).

(39) The fluorescence quantum yield of CNA is 0.8: Meyer, Y.; Astier, R.; Le Cleray, J. *J. Chem. Phys.* **1972**, *56*, 801.

(40) Arai, S.; Kira, A.; Imamura, M. *Phys. Chem.*, **1977**, *81*, 110-3.

solutions of TS with FN and DCA are similar (Table II), as expected if the reaction of TS^+ with O_2^- is rate limiting in both cases. Thus oxygen enhancement of the TS^+ decay rate is less pronounced in the case of DCA than FN. The initial yield of TS^+ is reduced by a factor of 1.4 in the presence of oxygen (Figure 5 and ref 4). This observation requires that oxygen-catalyzed intersystem crossing of the singlet geminate radical ion pair yields a triplet radical ion pair which does not dissociate to yield solvated TS^+ (Scheme II). This conclusion is consistent both with the large rate constant for homogeneous recombination of TS^+ with DCA^- and with the effect of oxygen on the quantum yield for CS formation.

Conclusions

The formation of free solvated *trans*-stilbene cation radicals as a consequence of photostimulated electron-transfer reactions in the TS/FN charge-transfer complex or from *trans*-stilbene to either $^1CNA^*$ or $^1DCA^*$ in acetonitrile solutions is established by our observations. The RR spectrum of the short-lived radical

cation is characterized by a ring $C=C$ stretching frequency at 1605 cm^{-1} and a frequency at 1285 cm^{-1} , which could be located mainly in the central part of the molecule. These frequencies are significantly different from those of neutral *trans*-stilbene or the *trans*-stilbene anion radical although the absorption spectra of both radical ions are almost identical. The *trans*-stilbene radical cations decay by homogeneous recombination of the radical ion pairs $TS^+ \cdot FN^-$, $TS^+ \cdot DCA^-$, or $TS^+ \cdot CNA^-$. Evidence for additional competitive reactions was obtained from the time-dependent intensities of the TS^+ RR bands. The reaction of TS^+ with fumaronitrile dimer anion radicals $(FN)_2^-$ leads to the formation of a triplex $(TS^+ \cdot (FN)_2^-)$, which decays to the ground-state molecules without the formation of 3TS and CS. In the presence of oxygen an additional fast decay route of the solvated TS^+ molecules is found, due to the reaction of TS^+ with O_2^- .

Acknowledgment. Financial support of the Deutsche Forschungsgemeinschaft and the National Science Foundation (CHE 8026020) is gratefully acknowledged. Travel expenses have been paid by NATO (Research Grant 1911).

Registry No. *trans*-Stilbene, 103-30-0; *trans*-stilbene anion radical, 34473-61-5; fumaronitrile dimer anion radical, 89399-26-8; superoxide ion, 11062-77-4; *trans*-stilbene cation radical, 59532-48-8; fumaronitrile, 764-42-1; 9-cyanoanthracene, 1210-12-4; 9,10-dicyanoanthracene, 1217-45-4.

- (41) Wong, P. C. *Can. J. Chem.* **1982**, *60*, 339-41.
 (42) Birks, J. B., Ed. "Organic Molecular Photophysics"; Wiley: New York, 1975; Vol. 2, p 534.
 (43) Weller, A. *Z. Phys. Chem. (Frankfurt am Main)* **1982**, *130*, 129-38.
 (44) Dobrowolski, D. C.; Ogilby, P. R.; Foote, C. S. *J. Phys. Chem.* **1983**, *87*, 2261-3.

Molecular Structure and Conformation of 1-Chloropropane As Determined by Gas Electron Diffraction and Microwave Spectroscopy

Kaoru Yamanouchi,[†] Masaaki Sugie,[‡] Harutoshi Takeo,[‡] Chi Matsumura,[‡] and Kozo Kuchitsu*[†]

Department of Chemistry, Faculty of Science, The University of Tokyo, Bunkyo-ku, Tokyo 113, Japan, and National Chemical Laboratory for Industry, Yatabe, Tsukuba-gun, Ibaraki 305, Japan

(Received: August 19, 1983)

The electron diffraction intensity and microwave spectra for 1-chloropropane have been measured. The A_0 constants of the *trans* conformer for the ^{35}Cl and ^{37}Cl species have been found to be 25 753.2 (2) and 25 737.3 (2) MHz, respectively. A least-squares analysis of the diffraction intensity and the rotational constants leads to the following r_g structure (bond lengths) and r_t structure (angles): $r(C-H) = 1.113$ (3) Å, $r(C-C) = 1.525$ (2) Å, $r(C-Cl) = 1.796$ (2) Å, $\angle C-C-C(g) = 113.9$ (5)°, $\angle C-C-C(t) = 111.3$ (13)°, $\angle C-C-Cl(g) = 112.2$ (6)°, $\angle C-C-Cl(t) = 111.3$ (7)°, and the dihedral angle $C-C-C-Cl(g) = 63.9$ (12)°, where g and t represent the *gauche* and *trans* conformers, respectively. The listed values are weighted averages of the two conformers unless specified. The abundance ratio of the *trans* conformer at room temperature is found to be 38 (3)%. The enthalpy difference, $\Delta H(g-t)$, is calculated to be -45 ± 70 cal/mol by using skeletal torsional frequencies for g and t measured in the present study, 133 (2) and 120 (2) cm^{-1} , respectively. The dipole moments are measured to be 2.02 (11) and 1.95 (6) D for g and t, respectively.

Introduction

Previous studies of 1-chloropropane by vibrational¹⁻³ and rotational^{4,5} spectroscopy and by gas electron diffraction⁶ have shown that the *gauche* and *trans* conformers (Figure 1) exist in the gas phase with practically no enthalpy difference. A molecular mechanics calculation by Meyer and Allinger⁷ gave $\Delta H(g-t) = 240$ cal/mol, while other semiempirical calculations predicted 167⁸ and -220 cal/mol.⁹

The bond lengths and angles for both conformers determined by gas electron diffraction were reported by Morino and Kuchitsu.⁶ In their analysis a number of parameters had to be assumed, particularly because none of the rotational constants were available at that time. Later, Sarachman⁴ reported the rotational constants

for both conformers except for the A_0 constant for the *trans* conformer.

Much attention has been paid to the ΔH of this molecule, because it is regarded as one of the starting points for conformational calculations.⁷⁻¹⁰ In view of the importance of this molecule in structural chemistry, we decided to reinvestigate the

- (1) C. Komaki, I. Ichishima, K. Kuratani, T. Miyazawa, T. Shimanouchi, and S. Mizushima, *Bull. Chem. Soc. Jpn.*, **28**, 330 (1955).
 (2) Y. Ogawa, S. Imazeki, H. Yamaguchi, H. Matsuura, I. Harada, and T. Shimanouchi, *Bull. Chem. Soc. Jpn.*, **51**, 784 (1978).
 (3) T. Tanabe and S. Saeki, *J. Mol. Struct.*, **27**, 79 (1975).
 (4) T. N. Sarachman, *J. Chem. Phys.*, **39**, 469 (1963).
 (5) V. K. Kaushik, *Spectrochim. Acta, Part A*, **33A**, 463 (1977).
 (6) Y. Morino and K. Kuchitsu, *J. Chem. Phys.*, **28**, 175 (1958).
 (7) A. Y. Meyer, N. L. Allinger, and Y. Yuh, *Isr. J. Chem.*, **20**, 57 (1980).
 (8) R. H. Boyd and L. Kesner, *J. Chem. Phys.*, **72**, 2179 (1980).
 (9) R. J. Abraham and R. Stölevik, *Chem. Phys. Lett.*, **77**, 181 (1981).
 (10) N. L. Allinger, private communication, 1982.

[†]The University of Tokyo.

[‡]National Chemical Laboratory for Industry.